
CMS Physics Analysis Summary

Contact: cms-pag-conveners-susy@cern.ch

2013/05/17

Search for RPV SUSY resonant second generation slepton production in same-sign dimuon events at $\sqrt{s} = 7$ TeV

The CMS Collaboration

Abstract

A search for resonant production of second generation sleptons ($\tilde{\mu}$, $\tilde{\nu}_\mu$) via the R-parity violating coupling λ'_{211} , with two same-sign muons and at least two jets in the final state is performed. While one muon is expected to be produced directly in the slepton decay, the second muon and at least two jets are produced in the subsequent decay of a neutralino or chargino originating from the resonant slepton. The analysis is based on the 2011 dataset of proton proton collisions at a centre of mass energy of $\sqrt{s} = 7$ TeV taken with the CMS detector, corresponding to an integrated luminosity of 4.98 fb^{-1} . The observation is in agreement with the expectation from Standard Model processes. Limits are set within the mSUGRA framework on the coupling λ'_{211} in the range of scalar masses m_0 up to 1.3 TeV and gaugino masses $m_{1/2}$ up to 1 TeV and interpreted in the $m_{\tilde{\mu}}, m_{\tilde{\chi}_1^0}$ mass plane.

1 Introduction

Supersymmetry (SUSY) [1, 2] is an attractive extension of the Standard Model because of coupling unification, dynamic electroweak symmetry breaking and a solution to the hierarchy problem. Constructing the most general minimal supersymmetric theory, one obtains lepton- and baryon-number violating terms in the superpotential [3]:

$$W_{LNV+BNV} = \epsilon_{ab} \left[\underbrace{\frac{1}{2} \lambda_{ijk} L_i^a L_j^b \bar{E}_k}_{LLE \text{ term}} + \underbrace{\lambda'_{ijk} L_i^a Q_j^{xb} \bar{D}_{kx}}_{LQD \text{ term}} \right] - \underbrace{\epsilon_{ab} \kappa^i L_i^a H_u^b}_{LH \text{ term}} + \underbrace{\frac{1}{2} \epsilon_{xyz} \lambda''_{ijk} \bar{U}_i^x \bar{D}_j^y \bar{D}_k^z}_{UDD \text{ term}} \quad (1)$$

Here, the coefficients λ, λ' and κ allow lepton number violation (LNV), whereas the coefficient λ'' allows baryon number violation (BNV). These terms in conjunction lead to rapid proton decay, which has not been observed in nature [4]. In order to keep the proton stable, an additional symmetry is introduced. The most common choice for this symmetry is R-parity, which forbids all lepton- and baryon-number violating terms. However, equally theoretically well-motivated symmetries can replace R-parity in order to prevent proton decay. In these scenarios R-parity is not conserved, and thus such models are dubbed "R-parity violating (RPV) supersymmetry". In RPV SUSY scenarios the lightest supersymmetric particle (LSP) is not stable and decays into Standard Model particles. This leads to signatures which we investigate in this study. Due to the decay of the LSP, the signature of RPV SUSY differs strongly from standard SUSY searches since it exhibits no missing energy due to an escaping neutralino, and thus limits from searches for R-parity conserving SUSY typically do not apply.

In this document we report on the search for resonant slepton production in a "baryon triality" (B_3) mSUGRA scenario [5, 6], where $\lambda'' = 0$. At the LHC, sleptons can be resonantly produced via the Yukawa coupling coefficient λ'_{ijk} of the trilinear LQD term in the RPV superpotential, c. f. equation (1), where $i = 1..3$ denotes the lepton generation and $j, k = 1..3$ denotes the quark generation. Since protons are used in the initial state, the contribution for $j, k = 1$ is dominant. Bounds on the first generation coupling λ'_{111} from neutrinoless double beta decay [3] motivate a search for second generation slepton production ($i = 2$). Single coupling dominance for λ'_{211} [3] is assumed such that contributions from other RPV couplings can be neglected.

Assuming λ'_{211} to be small, the slepton produced in the primary interaction decays predominantly into a muon/neutrino and neutralino/chargino, and the decay via λ'_{211} leading to a dijet final state can be neglected. Depending on the mass hierarchy of the sparticles, the subsequent R-parity conserving decay of the neutralino or chargino can lead to additional jets, leptons and/or neutrinos in the final state. The neutralino LSP decays in a three-body decay via the RPV coupling λ'_{211} to a muon and two jets, or to a neutrino and two jets, leading to a final state with at least two jets and zero, one or two muons. The lifetime of the neutralino LSP depends on the value of λ'_{211} , and the decay is effectively prompt for detection purposes for values $\lambda'_{211} > 10^{-6}$.

2 Search strategy

This search extends the results from a previous search by the DØ collaboration [7] and is complementary to searches for RPV SUSY by the LEP experiments [3]. The search concentrates on final states with two muons and at least two jets. Fig. 1 illustrates the simplest possible Feynman diagrams leading to this final state, which is experimentally interesting because the

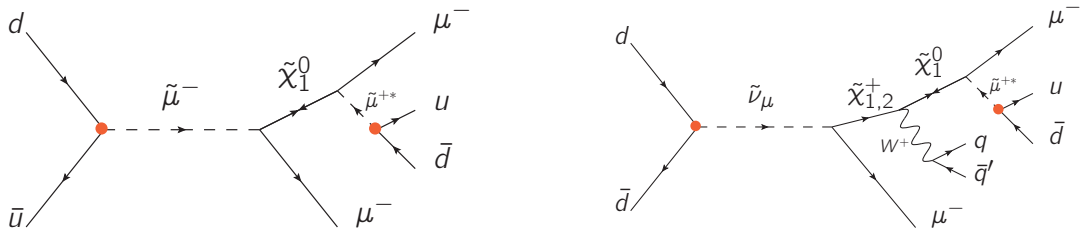


Figure 1: Resonant smuon (left) and sneutrino (right) production and typical decay chain into final states with two same-sign muons and at least two jets. The R-parity violating vertices are marked by a red filled circle.

presence of two muons allows to discriminate the signal from background processes. One of the muons is expected to be produced by the resonant slepton while the other muon and two quarks resulting in jets are expected to be produced in the subsequent decay of the neutralino LSP. Due to the Majorana nature of the LSP, the two muons have the same charge with about 50% probability, which allows to discriminate further against the background. Due to the larger valence u-quark content of the initial state protons the configuration with two positively charged muons is about twice as large as the configuration with two negatively charged muons. The kinematics of this signal is characterised by no missing transverse energy within the detector resolution. After selecting events with two same-sign muons, at least two jets, low amount of missing energy, no electrons and no b-jets, two main background components can be identified: low cross section backgrounds containing two prompt same-sign leptons such as production of multiple bosons, and backgrounds with high cross-section where leptons from semileptonic decays of c or b-hadrons or other charged particles are wrongly identified as prompt leptons, which are both called “fakes” for the purpose of this document. The “fake” backgrounds are estimated from the data. The observed events then are compared to the background by reconstructing the invariant mass of the slepton and neutralino/chargino.

This document is organised as follows: Section 3 describes the data sample and simulation of background processes. The event selection is presented in section 4. Section 5 describes how the backgrounds are estimated. Systematic uncertainties are evaluated in section 6, and the results of this search are presented in section 7. The document concludes with section 8.

3 Data and simulation samples

In this search, we use the entire 2011 dataset taken at $\sqrt{s} = 7$ TeV with the CMS detector based on dimuon triggers with various low transverse momentum requirements on the muons. The integrated luminosity corresponds to $\mathcal{L} = 4.98 \pm 0.11 \text{ fb}^{-1}$.

Simulated background samples for the production of QCD multi-jet, Drell-Yan, $W, W + \gamma$, top-pair production ($t\bar{t}, t\bar{t} + V$), double boson (VV) and triple boson (VVV) events, where $V = W, Z$ stands for a W or a Z boson, are generated with MADGRAPH [8] interfaced to the event generator PYTHIA 6 [9] for parton shower, hadronisation and underlying event. Single top quark production samples are generated with POWHEG [10–12]. We also use simulation for estimating contributions from rare processes such as $W^\pm W^\pm$ -production, double-parton scattering and $W\gamma^*$ production with an asymmetric internal photon conversion.

For the RPV resonant slepton signal production particle mass spectra have been generated with SoftSusy 3.1.7 [13, 14] under the premise of the mSUGRA model. The mass spectrum of produced particles is processed through Isajet 7.64 [15] to obtain the decay widths and branching

ratios needed in the subsequent event generation. The masses, decay widths and branching ratios of the obtained particles are fed into the Monte-Carlo event generator HERWIG 6.5 [16–18] using parton distribution functions CTEQ6L [19].

The RPV resonant slepton events have been exclusively generated with the LQD coupling $\lambda'_{211} = 0.01$. Since the production cross section scales with the square of the coupling for coupling values considered in this analysis, different λ'_{211} values can be adopted after simulation for the limit settings without loss of generality. We ensured that effects on the lifetime are small enough to consider the decay as prompt and changes to the event kinematics are negligible for all scaling values used in this analysis.

We consider 400 phase space points in the two dimensional interval of $50 \leq m_{1/2} \leq 1000$ GeV in 50 GeV steps and $100 \leq m_0 \leq 2000$ GeV in 100 GeV steps, with values of $\tan \beta = 20$, $\text{sgn}(\mu) = +1$, $A_0 = 0$, and $\lambda'_{211} = 0.01$ fixed. Some regions of this phase space exhibit non-convergent renormalisation group equations, tachyonic solutions, a $\tilde{\tau}$ LSP or fail to exhibit electroweak symmetry breaking. These regions are removed from further consideration, and the 354 remaining phase space points are simulated to derive model specific exclusion limits. For illustration purposes, we additionally evaluate the CMS benchmark points LM1 ($m_0 = 60$ GeV, $m_{1/2} = 250$ GeV), HM1 ($m_0 = 180$ GeV, $m_{1/2} = 850$ GeV), HM3 ($m_0 = 700$ GeV, $m_{1/2} = 800$ GeV), with common values $\tan \beta = 10$, $\text{sgn}(\mu) = +1$, $A_0 = 0$ [20].

Leading order cross sections for resonant slepton production have been computed by HERWIG 6.5 for the chosen coupling $\lambda'_{211} = 0.01$. The cross section ranges from 177 pb at lowest $m_0, m_{1/2}$ masses to about $2 \cdot 10^{-4}$ pb at highest $m_0, m_{1/2}$ masses. Next-to-leading order (NLO) k -factors have been derived using the prescription in [21] at each phase space point. The k -factors vary moderately over the entire considered phase space from 1.15 to 1.35.

The detector response is simulated with the GEANT4 [22] framework. The pileup distribution used during simulation is reweighted to the measured pileup distribution with 50 ns bunch spacing and out of time pileup contributions from previous bunch crossings by a three dimensional reweighting procedure [23], and corresponding jet energy corrections are applied [24].

4 Event selection

We select events passing High Level Trigger dimuon requirements containing two muons with transverse momentum thresholds varying between 6 and 17 GeV. Events are required to have at least one well reconstructed vertex within $\Delta z < 24$ cm around the nominal interaction point. Events that contain reconstructed electrons exceeding a transverse momentum of 30 GeV or high noise in the electromagnetic and hadronic calorimeter cells are discarded from the analysis.

The p_T -threshold for muons is optimised to retain high signal efficiency while keeping contributions from backgrounds small. To avoid turn-on effects, the muon p_T requirements are chosen above trigger thresholds where in average an efficiency of $92\% \pm 1\%$ is achieved. The resulting requirements are $p_T > 20$ GeV for the leading muon and $p_T > 15$ GeV for the second leading one. Muons have to be reconstructed both in the muon chambers and in the silicon tracker and reside in the pseudorapidity range of $|\eta| < 2.1$, avoiding endcap regions with high background contamination. Compared to the trigger requirements on the muons, a stricter muon identification is adopted [25] in order to reduce contributions from misidentified muons. An invariant mass of $M(\mu, \mu) > 15$ GeV is required to exclude events with J/ψ , Υ , low-mass Drell-Yan processes as well as photon conversions.

Muons are isolated from surrounding energy deposits by requiring $Iso_{rel} < 0.15$, where

$$Iso_{rel} = (Iso_{Trk} + Iso_{ECal} + Iso_{HCal}) / p_T^\mu \quad (2)$$

The values Iso_{Trk} , Iso_{ECal} and Iso_{HCal} are defined as the sum of all charged or neutral particle p_T inside a cone of $\Delta R < 0.3$ around the muon, excluding the muon itself, as measured by the silicon tracker, the electromagnetic or the hadronic calorimeter, respectively. We denote the isolated muon with the highest transverse momentum as μ_1 and the isolated muon with the second highest transverse momentum as μ_2 .

Jets with a transverse momentum of $p_T > 30 \text{ GeV}$ in a range of $|\eta| < 2.4$ are selected. Further jet identification quality requirements [26] are applied, and we require at least two jets in the event. b-jets are identified and vetoed with a Track Counting High Efficiency (TCHE) algorithm at medium working point [27]. The simulation of b-tagging is corrected to match the data by scaling the simulated efficiency to the measured efficiency obtained from QCD multi-jet events [28].

Further requirements on the reconstructed objects described above are applied. Events with a muon close to a jet by $\Delta R < 0.4$ are rejected to decrease the contribution of non-prompt muons. Furthermore, muons are required to originate from the same vertex by requiring $\Delta z(\mu_1, \mu_2) < 0.8 \text{ mm}$. Since no missing transverse energy (E_T^{miss}) is expected within the detector resolution, backgrounds such as $t\bar{t}$ production with neutrinos in the final state can be partially suppressed by requiring $E_T^{\text{miss}} < 50 \text{ GeV}$, where the E_T^{miss} is obtained by means of particle flow objects.

After applying these selection requirements, the dominant background is from Drell-Yan production, followed by $t\bar{t}$ production. At this stage, the Drell-Yan simulation is scaled to match the event yield in the Z-peak region in the invariant $m(\mu_1, \mu_2)$ mass distribution. The scale factor we obtain over the mass range from 80 to 100 GeV is $f_{sc} = 0.88$. The left plot of Fig. 2 shows

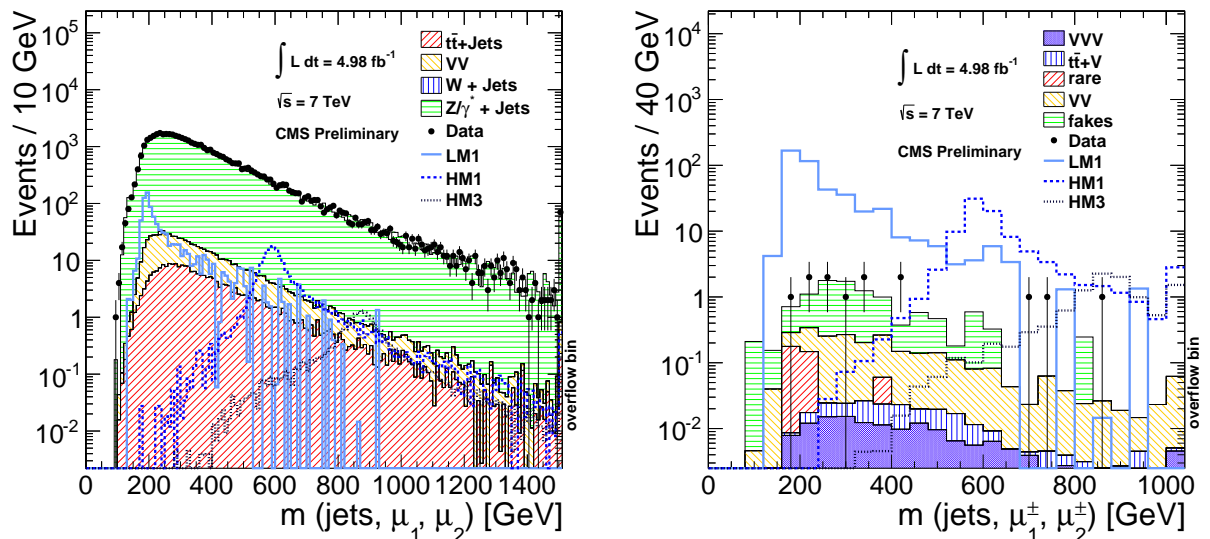


Figure 2: Invariant mass of the two muons and jets before (left) and after (right) applying the b-tag veto and same-sign muon requirement. Data are compared to the expectation from simulation (left) and measured backgrounds (right). Signal distributions are shown for three different kinematic configurations for a coupling value of $\lambda'_{211} = 0.01$.

the invariant mass distribution of the two muons and jets after the scaling has been applied, representing the mass of the slepton resonantly produced in the primary interaction. A good

agreement between data and simulation is observed. The dominant Drell-Yan background is drastically reduced by requiring two same-sign muons. After this requirement, $t\bar{t}$ production with one of the two same-sign muons either misidentified or originating from a semi-leptonic b -decay constitutes the main background. It is reduced by further rejecting events with identified b -jets. The resulting invariant mass distribution is shown in the right plot of Fig. 2. Contributions from faked leptons have been estimated with a data-driven method described below, and predictions for rare processes with prompt leptons are taken from simulation.

The signal selection efficiency has been determined from simulation. Both the resonant production of a smuon as well as a muon sneutrino can lead to a same-sign two-muon final state. However, the majority of final states contain neutrinos instead of muons and thus efficiency is lost by requiring two muons. Additional 50% efficiency is lost by requiring same-sign muons. The efficiency is thus a few percent for most of the considered phase space. For low values of $m_{1/2}$, the neutralino is very light, boosted, and its decay products do not match the isolation criteria. This leads to small signal efficiencies. Since the muon originating from the slepton decay is not sufficiently energetic, this search lacks sensitivity when the neutralino or chargino mass is close to that of the slepton. Because efficiencies are small for parts of the phase space, they have been computed together with their uncertainties making use of the Wilson score interval [29].

5 Background estimate

After the selection has been performed, very little background remains from Standard Model processes. The most prevalent background source arises from non-prompt leptons in the decay of c - or b -hadrons or misidentified leptons. This background is difficult to model in simulation and thus is estimated from the data.

To this end, the muon isolation requirement is loosened from the “tight” requirement $Iso_{rel} < 0.15$ to the “loose” requirement $Iso_{rel} < 0.4$ in order to enrich non-prompt and misidentified muon contributions. Then, events with exactly one such loose lepton are used to measure the probability $F_R = T/L$, i.e. the fraction of tight leptons T in the loose lepton sample L . The loose lepton sample is enriched in QCD multi-jet events. Events with prompt leptons from $W+jets$ are rejected by building a transverse mass hypothesis m_T of the loose lepton p_T and the missing energy E_T^{miss} by requiring $m_T < 40$ GeV. Drell-Yan events are rejected by further loosening the muon identification requirements and requiring the invariant mass of any two muons to be outside of the interval $71 \dots 111$ GeV. However, a small remaining contribution of prompt leptons from Drell-Yan and $t\bar{t}$ production remains. This contribution is estimated from simulation and subtracted for the calculation of F_R . The measurement of F_R is performed in bins of p_T and η corresponding to the detector resolution.

The contribution of non-prompt and fake leptons in the analysis then is estimated from an event sample where one tight lepton is replaced by one lepton which is loose but not passing tight identification requirements. By applying a weight factor $w = F_R/(1 - F_R)$ to this event, the contribution of events with one prompt lepton and one fake lepton (e.g. from semileptonic $t\bar{t}$ background) to the analysis sample is estimated. This contribution is called “single-fake”, and we measure $N_{SF} = 9.7 \pm 1.6$ (stat.) “single-fake” events, where the stated uncertainty arises from the limited size of the loose muon sample.

Events with two fake leptons can also pass the selection criteria although the probability is small. This case is non-negligible for QCD multi-jet events due to their high cross-section. The contribution can be estimated by selecting another sample where both tight muons in the

analysis are replaced by loose (but not tight) muons and applying w for each muon individually. This contribution is called “double-fake”, and we measure and $N_{DF} = 1.5 \pm 0.3$ (stat.) “double-fake” events.

Since the double-fake estimate by construction is contained in the single-fake estimate twice, the resulting fake contribution is $N_{fakes} = 8.2 \pm 1.6$ (stat.) events. The fake rate contribution is additionally determined in a signal-free control region (CR) defined by inversion of the E_T^{miss} requirement in the selection, leading to $N_{SF}^{\text{CR}} = 6.5 \pm 1.2$, $N_{DF}^{\text{CR}} = 0.2 \pm 0.1$ and thus $N_{fakes}^{\text{CR}} = 5.6 \pm 1.1$ (stat) ± 1.7 (syst.), again with statistical uncertainties due to the limited size of the loose muon sample. By adding backgrounds that contain two real same-sign muons and thus are not predicted by the fake rate method ($t\bar{t} + V$, VVV , ... with $V = Z, WW$), we arrive at $N_{back}^{\text{CR}} = 11.7 \pm 3.6$ (stat.) ± 1.9 (syst.). This is compatible with the $N_{data}^{\text{CR}} = 8$ data events within the stated uncertainty and assures confidence in the background determination method.

The data-driven background estimate method is validated using only simulated events. To this end, the T/L ratio is estimated from simulated QCD multi-jet events. The prediction for $t\bar{t}$ production from the T/L ratio method is then compared to the Monte-Carlo prediction for $t\bar{t}$ production in the selected default analysis sample. Good agreement is obtained with 2.4 ± 0.2 events after selection compared to 2.1 ± 0.1 events predicted from the T/L ratio method.

There are only a few Standard Model processes with low cross-sections that contain two same-sign muons and least two jets. These backgrounds are estimated from simulation. We consider double-boson, triple-boson and $t\bar{t} + V$ production that constitute an irreducible background. Also, rare processes such as double parton interactions or two interactions in one bunch crossing can lead to the same final state and are estimated from simulation.

6 Systematic uncertainties

We investigate several sources of systematic uncertainties on the event sample after selection. Reconstructed object uncertainties of Jet Energy Scale (JES) and resolution (JER) as well as muon energy scale and resolution are taken into account. Due to the fact that E_T^{miss} is used in the event selection, all object energy variations have to be propagated into E_T^{miss} . JES uncertainties have been evaluated following the procedure of [24]. The impact on the number of selected events is 2% for background and up to 10% for signal, depending on the choice of mSUGRA phase space point.

The Jet Energy Resolution in simulation is better than in data. The simulation has been corrected for this difference. Systematic uncertainties arise from matching ambiguities between jets of generated final state particles and reconstructed particle flow jets. The influence on the event selection has been found to be less than 1% for background and signal. The energy scale of muons was shifted and their resolution smeared with a Gaussian function following [25]. The resultant uncertainties have been found to be negligible.

Uncertainties specific to luminosity, reweighting and cross section are evaluated as follows: an error of 2.2% is assigned to the integrated luminosity [30], resulting in $\mathcal{L} = 4.98 \pm 0.11 \text{ fb}^{-1}$. The systematic uncertainty on the pileup reweighting procedure for simulated events [23] has been obtained by varying the number of interactions per event by $\pm 5\%$. The resulting effect is $\pm 1\%$ for background and $\pm 4\%$ for signal. Evaluation of PDF and α_s uncertainties has been accomplished following the PDF4LHC procedure [31] making use of the PDF sets CT10, MSTW2008 and NNPDF2.1. The influence on background is $\pm 6\%$. On the signal the influence is $\pm 5\%$ because the PDF dependence is smaller in the NLO calculation.

The parameters of the b-tagging correction procedure are varied by the uncertainties found when computing the correction factors [28]. The resulting uncertainty for the background is less than one percent. For the signal the uncertainty goes up to 6% depending on the parameter point.

To obtain systematic uncertainties on the background estimate for fake leptons, the relative muon isolation criterion and the selection criteria for enriching the QCD multi-jet contribution while suppressing prompt leptons have been varied and for each variation N_{fakes} is re-evaluated. From the results of these variations, a systematic uncertainty of 30% on the event yield is attributed to the method.

Cross section uncertainties for the signal are 5% due to scale variation and 5% for PDF uncertainties. A SUSY model-dependent interpretation gives rise to additional 7% uncertainty due to SUSY QCD corrections at NLO. By adding in quadrature, a total uncertainty of 10% on the signal cross-section is taken into account in the limits derivation procedure. For the simulated backgrounds we consider NNLO, NNLL and NLO cross-sections with corresponding uncertainties where available, and assign a 50% uncertainty to rare backgrounds, $t\bar{t} + V$, and triple boson production.

7 Results and interpretation

After the selection requirements we observe 13 candidate events (see Figure 2 right). The data-driven estimate for fake muon backgrounds yields $N_{fakes} = 8.3 \pm 1.6$ (stat.) ± 2.5 (syst.) events. Predictions from simulation for the remaining backgrounds yield $N_{\ell\ell} = 2.4 \pm 0.1$ (stat.) ± 1.0 (syst.), such that the total expected background amounts to $N_{background} = 10.7 \pm 1.6$ (stat.) ± 3.0 (syst.) events. Good agreement is thus observed between data and the prediction from simulation and data-driven background.

Further insight into the data can be obtained by studying the two-dimensional distribution $m_{\tilde{\mu}}$ vs. $m_{\tilde{\chi}}$, where a peak is expected for the signal. In order to reconstruct the mass of the neutralino (or chargino) from the slepton decay, one muon needs to be identified coming from

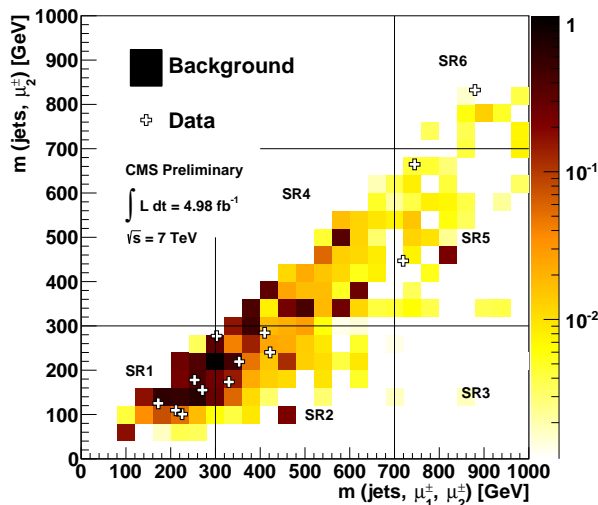


Figure 3: Distribution of $m_{\tilde{\mu}} = m(jets, \mu_1^\pm, \mu_2^\pm)$ vs. $m_{\tilde{\chi}} = m(jets, \mu_1^\pm, \mu_2^\pm)$ for the events selected in data compared to the total background contribution. The crosses represent the data points and the coloured squares show the expectation from Standard Model backgrounds.

Table 1: Event yields with systematic uncertainties after selection requirements, broken down in individual Standard Model background contributions, with observed 95% C.L. limits on the number of signal events N_{sig} in total and for each signal region.

process	totals	SR1	SR2	SR3
VVV	0.15 ± 0.08	0.043 ± 0.022	0.054 ± 0.028	<0.001
tt+V	0.11 ± 0.06	0.019 ± 0.010	0.038 ± 0.020	0
rare	0.36 ± 0.26	0.32 ± 0.24	0.042 ± 0.042	<0.001
VV	2.1 ± 1.1	0.69 ± 0.35	0.68 ± 0.34	0.003 ± 0.002
fakes	8.2 ± 3.0	3.5 ± 1.6	1.9 ± 1.0	<0.001
Σ	10.9 ± 3.4	4.6 ± 1.6	2.7 ± 1.1	0.003 ± 0.002
data	13	5	5	0
95% C.L. limit on N_{sig}	11.3	6.9	8.0	2.8
process		SR4	SR5	SR6
VVV		0.036 ± 0.018	0.010 ± 0.005	0.007 ± 0.004
tt+V		0.044 ± 0.023	0.006 ± 0.004	0.006 ± 0.004
rare		<0.001	<0.001	<0.001
VV		0.49 ± 0.25	0.15 ± 0.08	0.093 ± 0.050
fakes		2.5 ± 1.2	0.22 ± 0.23	<0.001
Σ		3.1 ± 1.2	0.39 ± 0.25	0.11 ± 0.05
data		0	2	1
95% C.L. limit on N_{sig}		2.9	6.0	4.6

the slepton decay. Although there are in principle two choices, the muon from the slepton decay is in most regions of the parameter space higher energetic than the muon from the LSP decay and thus can be identified as μ_1 . Therefore, the compatibility of observed data events with the background estimation can be examined further by means of the two-dimensional distribution $m_{\tilde{\mu}} = m(\text{jets}, \mu_1^\pm, \mu_2^\pm)$ vs. $m_{\tilde{\chi}} = m(\text{jets}, \mu_2^\pm)$ in Fig. 3. The observed events in the data are compatible with the background expectation; no special structure can be observed. The parameter space is subdivided into six signal regions SR1 – SR6, corresponding to low, medium and high mass for the slepton and the neutralino, respectively. These regions, indicated in Fig. 3, are sensitive to different combinations of slepton and neutralino masses. The bin width is chosen such that the expected contribution from a signal can fit approximately into a single bin, increasing the sensitivity for detecting a signal. The corresponding event yield for the six regions is given in Table 1.

Since the number of events from Standard Model backgrounds and data agree, there is no evidence for a signal. We interpret this result by providing three types of limits: One model-independent limit on the number of excess events, and two limits on the coupling parameter λ'_{211} for resonant production of second generation sleptons in the baryon triality model, the first as a function of the SUSY parameters m_0 and $m_{1/2}$, and the second as a function of the neutralino mass $m_{\tilde{\chi}_1^0}$ and the smuon mass $m_{\tilde{\mu}}$. We use the LHC-style [32] CL_s method [33] to derive limits. As a test statistic, a profile Likelihood [4] for a multi-bin Poisson counting experiment is used. The systematic uncertainties are modelled with log-normal distributions. All limits are set at the 95% confidence level.

We determine a model-independent limit on the number of excess events N_{sig} from a possible signal with respect to the predicted background after all selection requirements. We provide this limit for the observed final state overall, i.e. using the total yield of the selection, and in

the six signal regions individually. In the latter case, the assumption is that a potential signal only appears in one of the bins, and we thus neglect correlations with the observations in other bins. Taking the corresponding statistical and systematic uncertainties into account, we arrive at the limits listed in Table 1.

Figure 4 shows the expected upper limits on the λ'_{211} coupling strength within the baryon triality model as a function of the mSUGRA mass scales $m_{1/2}$ and m_0 in the upper plot and the corresponding measured upper limits in the centre plot, for $A_0 = 0$, $\text{sign}(\mu) = +1$ and $\tan \beta = 20$. The bottom plot shows the mSUGRA limits expressed in the parameter space of the neutralino mass $m_{\tilde{\chi}_1^0}$ and smuon mass $m_{\tilde{\mu}}$. The limits expand the previously reachable phase space explored by the DØ experiment [7] considerably.

8 Conclusions

We present a search for resonant production of sleptons ($\tilde{\mu}, \tilde{\nu}_\mu$) via the R-parity violating coupling λ'_{211} with two like-sign muons and at least two jets in the final state. The kinematics of the signal is characterised by no missing transverse energy within the detector resolution. The search is based on the 2011 dataset with an integrated luminosity of $\mathcal{L} = 4.98 \text{ fb}^{-1}$, recorded with the CMS detector in proton proton collisions at a centre of mass energy of $\sqrt{s} = 7 \text{ TeV}$. The observed number of events agrees with the Standard Model prediction and we establish most stringent limits to date on the coupling λ'_{211} in the range of scalar masses m_0 up to 1.3 TeV and gaugino masses $m_{1/2}$ up to 1 TeV. We also present these limits in the two-dimensional phase space of neutralino mass $m_{\tilde{\chi}_1^0}$ and smuon mass $m_{\tilde{\mu}}$. Compared to previous measurements from the DØ experiment [7], we extend the excluded phase space considerably.

References

- [1] H. P. Nilles, “Supersymmetry, Supergravity and Particle Physics”, *Phys. Rept.* **110** (1984) 1, doi:10.1016/0370-1573(84)90008-5.
- [2] H. E. Haber and G. L. Kane, “The Search for Supersymmetry: Probing Physics Beyond the Standard Model”, *Phys. Rept.* **117** (1985) 75, doi:10.1016/0370-1573(85)90051-1.
- [3] R. Barbier et al., “R-parity violating supersymmetry”, *Phys. Rept.* **420** (2005) 1–202, doi:10.1016/j.physrep.2005.08.006, arXiv:hep-ph/0406039.
- [4] Particle Data Group Collaboration, “Review of particle physics”, *Phys. Rev.* **D86** (2012) 010001, doi:10.1103/PhysRevD.86.010001.
- [5] L. E. Ibáñez and G. Ross, “Discrete gauge symmetries and the origin of baryon and lepton number conservation in supersymmetric versions of the standard model”, *Nucl. Phys. B* **368** (1992) 3–37, doi:10.1016/0550-3213(92)90195-H.
- [6] H. K. Dreiner, C. Luhn, and M. Thormeier, “What is the discrete gauge symmetry of the minimal supersymmetric standard model”, *Phys. Rev. D* **73** (2006) 075007, doi:10.1103/PhysRevD.73.075007, arXiv:0512163.
- [7] DØ Collaboration, “Search for Resonant Second Generation Slepton Production at the Fermilab Tevatron”, *Phys. Rev. Lett.* **97** (2006) 111801, doi:10.1103/PhysRevLett.97.111801, arXiv:0605010.

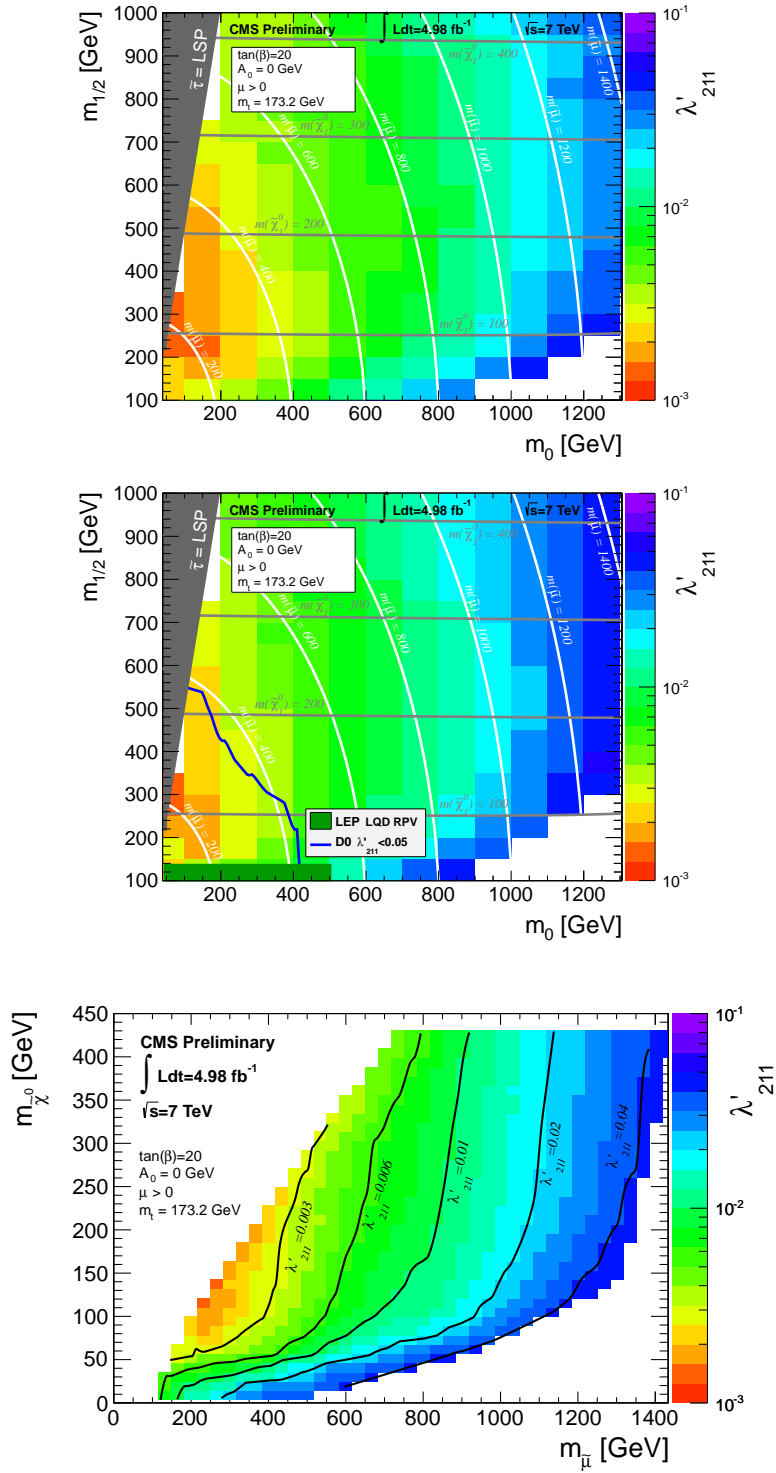


Figure 4: Expected (top) and observed (centre) 95% CL upper limits on λ'_{211} as a function of m_0 and $m_{1/2}$ for $A_0 = 0$, $\text{sign}(\mu) = +1$ and $\tan \beta = 20$. The bottom plot shows the mSUGRA limits expressed in the parameter space of the neutralino mass $m_{\tilde{\chi}_1^0}$ and smuon mass $m_{\tilde{\mu}}$.

- [8] F. Maltoni and T. Stelzer, "MadEvent: Automatic event generation with MadGraph", *JHEP* **02** (2003) 027, doi:10.1088/1126-6708/2003/02/027, arXiv:0208156.
- [9] T. Sjostrand, S. Mrenna, and P. Z. Skands, "PYTHIA 6.4 Physics and Manual", *JHEP* **05** (2006) 026, doi:10.1088/1126-6708/2006/05/026, arXiv:0603175.
- [10] S. Alioli et al., "NLO vector-boson production matched with shower in POWHEG", *JHEP* **07** (2008) 060, doi:doi:10.1088/1126-6708/2008/07/060, arXiv:0805.4802.
- [11] P. Nason, "A new method for combining NLO QCD with shower Monte Carlo algorithms", *JHEP* **11** (2004) 040, doi:doi:10.1088/1126-6708/2004/11/040, arXiv:0409146.
- [12] S. Frixione, P. Nason, and C. Oleari, "Matching NLO QCD computations with Parton Shower simulations: the POWHEG method", *JHEP* **11** (2007) 070, doi:doi:10.1088/1126-6708/2007/11/070, arXiv:0709.2092.
- [13] B. C. Allanach, "SOFTSUSY: a program for calculating supersymmetric spectra", *Comput. Phys. Commun.* **143** (2002) 305, doi:10.1016/S0010-4655(01)00460-X.
- [14] B. C. Allanach and M. Bernhardt, "Including R-parity violation in the numerical computation of the spectrum of the minimal supersymmetric standard model: SOFTSUSY", *Comput. Phys. Commun.* **181** (2010) 232, doi:10.1016/j.cpc.2009.09.015.
- [15] H. Baer et al., "ISAJET 7.69: A Monte Carlo Event Generator for pp , $\bar{p}p$, and e^+e^- Reactions", arXiv:0312045.
- [16] G. Marchesini et al., "Herwig, a Monte Carlo event generator for simulating Hadron Emmission Reactions with Interfering Gluons", *Comput. Phys. Commun.* **67** (1992) 465.
- [17] G. Corcella et al., "HERWIG 6.5: an event generator for Hadron Emission Reactions With Interfering Gluons (including supersymmetric processes)", *JHEP* **0101** (2001) 010, doi:10.1088/1126-6708/2001/01/010.
- [18] S. Moretti et al., "Implementation of supersymmetric processes in the HERWIG event generator", *JHEP* **0204** (2002) 028, doi:10.1088/1126-6708/2002/04/028.
- [19] J. Pumplin et al., "New Generation of Parton Distributions with Uncertainties from Global QCD Analysis", *JHEP* **0207** (2002) 012, doi:10.1088/1126-6708/2002/07/012, arXiv:0201195.
- [20] CMS Collaboration, "CMS Physics : Technical Design Report Volume 2: Physics Performance", *J. Phys. G* **34** (2007) 995-1579 (2007).
- [21] H. K. Dreiner et al., "Supersymmetric NLO QCD Corrections to Resonant Slepton Production and Signals at the Tevatron and the LHC", *Phys. Rev. D* **75:035003** (2007) doi:10.1103/PhysRevD.75.035003.
- [22] S. Agostinelli et al., "Geant4 - A Simulation Toolkit", *Nucl. Instr. and Meth. A* **506** (2003) 250, doi:10.1016/S0168-9002(03)01368-8.
- [23] CMS Collaboration, "PileupInformation", <https://twiki.cern.ch/twiki/bin/view/CMS/PileupInformation> (2011).

- [24] CMS Collaboration, “Determination of Jet Energy Calibration and Transverse Momentum Resolution in CMS”, *JINST* **6** (2011) doi:10.1088/1748-0221/6/11/P11002.
- [25] CMS Collaboration, “Performance of the CMS muon detector with pp collisions $\sqrt{s} = 7$ TeV/ c^2 at the LHC”, *CMS Physics Analysis Summary* (2010), no. CMS-PAS-MUO-10-002,.
- [26] CMS Collaboration, “Jet Performance in pp Collisions at $\sqrt{s} = 7$ TeV”, *CMS Physics Analysis Summary* (2010), no. CMS-PAS-JME-10-003,.
- [27] CMS Collaboration, “ b -Jet Identification at the CMS experiment”, *CMS Physics Analysis Summary* (2011), no. CMS-PAS-BTV-11-004,.
- [28] CMS Collaboration, “Identification of b -quark jets with the CMS experiment”, arXiv:1211.4462.
- [29] R. D. Cousins, K. E. Hymes, and J. Tucker, “Frequentist evaluation of intervals estimated for a binomial parameter and for the ratio of Poisson means”, *Nuclear Instruments and Methods in Physics Research Section A: Accelerators, Spectrometers, Detectors and Associated Equipment* **612** (2010), no. 2, 388 – 398, doi:10.1016/j.nima.2009.10.156, arXiv:0905.3831.
- [30] CMS Collaboration, “Absolute Calibration of the Luminosity Measurement at CMS: Winter 2012 Update”, *CMS Physics Analysis Summary* (2012), no. CMS-PAS-SMP-12-008,.
- [31] PDF4LHC Group, “Recommendation for LHC cross section calculations”, arXiv:1101.0538.
- [32] ATLAS and CMS Collaboration, “Procedure for the LHC Higgs boson search combination in Summer 2011”, *Technical Report* (2011), no. CMS-NOTE-2011-005,.
- [33] T. Junk, “Confidence Level Computation for Combining Searches with Small Statistics”, *Nucl. Instrum. Meth. A* **434** (1999) 435, doi:10.1016/S0168-9002(99)00498-2, arXiv:9902006.